ACS Photonics

Article

Cite This: ACS Photonics XXXX, XXX, XXX−XXX

pubs.acs.org/journal/apchd5

Modeling Molecular Orientation Effects in Dye-Coated Nanostructures Using a Thin-Shell Approximation of Mie Theory for Radially Anisotropic Media

Chhayly Tang,* Baptiste Auguié, and Eric C. Le Ru*

The MacDiarmid Institute for Advanced Materials and Nanotechnology, School of Chemical and Physical Sciences, Victoria University of Wellington, PO Box 600, Wellington 6140, New Zealand

Supporting Information

ABSTRACT: We here develop a thin-shell approximation of the Mie scattering problem for a spherical core−shell structure with radial anisotropy in the shell. The solution of the full anisotropic Mie theory requires the computation of Bessel functions of complex orders, which has severely limited its application to relevant problems. The proposed thin-shell approximation removes this hurdle and is of a similar complexity to the isotropic Mie theory. We show that the predictions agree with those of the full anisotropic theory for nanoparticles with a shell thickness of the order of 1 nm or less. The approximation is therefore of great relevance to calculations of the optical properties of adsorbed molecular monolayers, for example, the optical response of dye-coated nanoparticles. In this context, we also propose a simple effective medium shell model to account for the radial anisotropy of a dye layer arising from a preferred adsorption geometry, for example, in-plane or out-of-plane. We show that the model agrees with the predictions of a simple microscopic model, but provides additional insights on how the molecular orientation in the dye layer affects its interaction with the nanoparticle, for example, with plasmon resonance of metallic particles. These simple thin-shell approximation and effective medium anisotropic shell models pave the way for further theoretical understanding of orientation and anisotropic effects in the context of dye-plasmon resonance coupling.

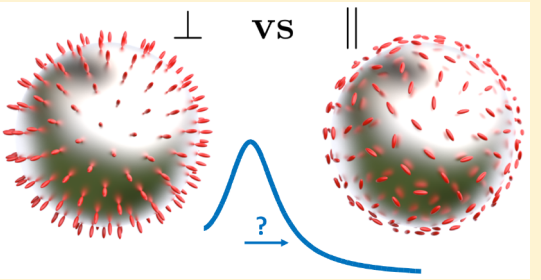

KEYWORDS: *Mie theory, optical anisotropy, nanoshells, molecular plasmonics, anisotropic dielectric function, effective-medium theory*

Recent progress in nano-optics, enabled in part by advanced nanofabrication techniques, but also driven by promising emerging applications, has led to a renewed interest in the theoretical modeling of light scattering by nanoparticles.[1,2] The electromagnetic theory of light scattering is commonly applied to isotropic media, where the dielectric functions of the media are the same in all directions. However, there are many relevant situations where this assumption is not justified and extensions to anisotropic media have therefore been developed, for example, in the context of reflection/refraction at interfaces.[3] For scattering by a finite object (such as nano- or microparticles), Mie theory provides a rigorous solution of the electromagnetic problem for objects with spherical symmetry such as spheres and spherical multilayers.[1,4] It has, for example, been used extensively to study the optical properties of nanoparticles, for instance, the plasmon resonances of metallic nanoparticles and core−shell structures.[5,6] Core−shell spherical nanostructures have been produced from a wide variety of materials, and the electromagnetic interaction between light and such multilayered structures can give rise to a wide variety of interesting functionalities, notably through the excitation of surface waves.[7−10]

The extension of Mie theory to radially anisotropic media was developed almost 50 years ago by Roth and Dignam,[11] and has been used, for example, to study the influence of anisotropy on plasmon resonances.[12,13] We will here focus on the special case of a core−shell structure with a radially anisotropic response in the shell only, as depicted in Figure 1. This configuration is particularly relevant to many recent works with dye-coated core−shell nanostructures, which have become a prototypical platform to study the interaction between plasmon and molecular resonances in either the weak or strong coupling regimes.[9,14−27] Mie theory has been used to understand the optical properties of dye-coated particles using effective medium theory,[28] where the dye layer is treated as a continuum medium with an effective dielectric function.[29] However, many studies to date have ignored the intrinsically anisotropic response of adsorbed dye layers, which arises from the fact that many dyes have a strongly uniaxial optical response (typically along the main chromophore axis) and tend to adsorb with a preferred orientation[30] (e.g., in-plane, perpendicular, or oblique). The first aim of this paper is to

Received: September 5, 2018
Published: October 17, 2018

DOI: 10.1021/acsphotonics.8b01251
ACS Photonics XXXX, XXX, XXX−XXX

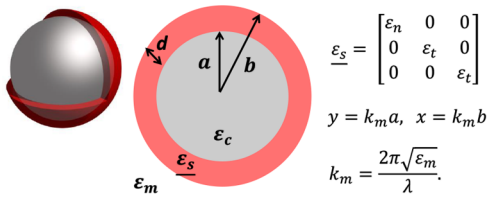

Figure 1. Schematic of the problem: a sphere of radius a and isotropic dielectric function ε_c (possibly complex and wavelength-dependent) is surrounded by a spherical shell of thickness $d = b - a$ with anisotropic properties described by a tensorial dielectric function $\underline{\varepsilon}_s$ and embedded in a nonabsorbing medium of dielectric constant ε_m (real). $\underline{\varepsilon}_s$ is assumed diagonal in the spherical basis with its normal (ε_n) and tangential (ε_t) components possibly both complex and wavelength-dependent.

show that the formalism developed by Roth and Dignam is well suited to account for these anisotropic effects within the macroscopic approach of continuous electrodynamics. It will therefore extend previous studies carried out in the quasi-static approximation.[30−32]

It should be noted, however, that this solution is more numerically challenging than the standard Mie theory, as it involves the use of Bessel functions of irrational or complex orders, in addition to the standard spherical Bessel functions (which are Bessel of half-integer order) of Mie theory. Complex-order Bessel functions are not built-in in many standard computing software (such as Matlab for example), which may have limited the uptake of this theoretical approach to model relevant experimental problems. One exception to this is the case of bubbles or vesicles, for which the dielectric function is the same inside and outside the shell ($\varepsilon_c = \varepsilon_m$). For this special case, Lange and Aragon[33] obtained simple approximations valid in the limit of thin shells ($d = b - a \ll a$), which no longer require the computation of Bessel functions of complex order. This simplified theory can be used in many applications, but it cannot be applied to core−shell nanoparticle/dye systems, where the inside and outside media are different. The second aim of this paper is therefore to obtain a more general form of this thin-anisotropic-shell approximation, valid for a general core material. We will show that this new solution does not involve complex order Bessel functions and is therefore no more numerically challenging than standard Mie theory. The validity of this approximation is assessed by comparing its predictions to the full anisotropic theory of Roth and Dignam[11] and shown to agree extremely well for shells of thickness typical of a molecular monolayer (of the order of 1 nm or less).

These results can therefore be readily used, for example, in theoretical studies of dye-coated nanoparticles. We illustrate this by calculating the optical properties of metallic nanoparticles coated with dyes at submonolayer coverage, within an effective medium approximation generalized to account for the anisotropy of the dye response. Strong orientation and anisotropic effects are evidenced and the predictions are compared with a microscopic model considering an individual dye as a polarizable dipole. This work highlights the importance of orientation effects in plasmon/dye interactions and provides a simple anisotropic model to predict them beyond the currently used isotropic models.

GENERAL MIE THEORY FOR AN ANISOTROPIC SHELL

We consider the light scattering problem by a radially anisotropic core−shell structure as depicted in Figure 1. A sphere of a radius a (which we will later choose as metallic) is covered by a thin spherical shell of thickness $d = b - a$ (typically a dye layer) and embedded in a nonabsorbing medium (typically air or water). The dielectric functions of the outside and inside media are assumed isotropic are denoted ε_m and ε_c, respectively. The spherical shell is assumed to have an anisotropic response characterized by a dielectric tensor, $\underline{\varepsilon}_s$. As in ref 11, we restrict ourselves to the much simpler case of radial anisotropy where the dielectric tensor $\underline{\varepsilon}_s$ is diagonal in the spherical basis with a radial component, ε_n, and a tangential component, ε_t. This situation is the most relevant in experiments where molecules are adsorbed with orientation defined with respect to the local surface, that is, perpendicular or tangential. It is a very common restriction in theoretical treatment and the optical response of such anisotropic systems has been called "systropic".[34]

The solution of the problem was fully derived in ref 11, and we only summarize below the final results. The field solutions are given as in Mie theory as series, from which standard optical properties can be derived. The extinction, scattering, and absorption cross sections in particular take the same form as in Mie theory, explicitly:

$$C_{\text{ext}} = \frac{2\pi}{k_m^2} \sum_{n=1}^{\infty} (2n+1)\text{Re}(\Gamma_n + \Delta_n) \tag{1}$$

$$C_{\text{sca}} = \frac{2\pi}{k_m^2} \sum_{n=1}^{\infty} (2n+1)(|\Gamma_n|^2 + |\Delta_n|^2) \tag{2}$$

$$C_{\text{abs}} = C_{\text{ext}} - C_{\text{sca}} \tag{3}$$

where $k_m = 2\pi\sqrt{\varepsilon_m}/\lambda$ and Γ_n and Δ_n are the Mie scattering coefficients, which are functions of the relative indices of refraction $s_c = \sqrt{\varepsilon_c}/\sqrt{\varepsilon_m}$ and $s_t = \sqrt{\varepsilon_t}/\sqrt{\varepsilon_m}$ and the size parameters $x = k_m b$ and $y = k_m a$.

For an anisotropic spherical shell, Roth and Dignam[11] showed that

$$\Gamma_n = -\frac{[\psi\psi]_{n,x}^{m,t}[\chi\psi]_{n,y}^{m,c} - [\chi\psi]_{n,x}^{m,t}[\psi\psi]_{n,y}^{m,c}}{[\psi\xi]_{n,x}^{m,t}[\chi\psi]_{n,y}^{m,c} - [\chi\xi]_{n,x}^{m,t}[\psi\psi]_{n,y}^{m,c}} \tag{4}$$

$$\Delta_n = -\frac{[\psi\psi]_{n,x}^{e,t}[\chi\psi]_{n,y}^{e,c} - [\chi\psi]_{n,x}^{e,t}[\psi\psi]_{n,y}^{e,c}}{[\psi\xi]_{n,x}^{e,t}[\chi\psi]_{n,y}^{e,c} - [\chi\xi]_{n,x}^{e,t}[\psi\psi]_{n,y}^{e,c}} \tag{5}$$

where

$$\begin{aligned}
[\Lambda\psi]_{n,y}^{m,c} &= s_c\Lambda_n(s_t y)\psi_n'(s_c y) - s_t\Lambda_n'(s_t y)\psi_n(s_c y), \\
[\Lambda\psi]_{n,y}^{e,c} &= s_c\Lambda_w'(s_t y)\psi_n(s_c y) - s_t\Lambda_w(s_t y)\psi_n'(s_c y), \\
[\Lambda\Omega]_{n,x}^{m,t} &= s_t\Lambda_n'(s_t x)\Omega_n(x) - \Lambda_n(s_t x)\Omega_n'(x), \\
[\Lambda\Omega]_{n,x}^{e,t} &= s_t\Lambda_w(s_t x)\Omega_n'(x) - \Lambda_w'(s_t x)\Omega_n(x), \\
\text{with} \quad \Lambda &= \psi \quad \text{or} \quad \chi, \quad \text{and} \quad \Omega = \psi \quad \text{or} \quad \xi
\end{aligned} \tag{6}$$

ψ_n and χ_n are the regular and irregular Riccati-Bessel functions of integer order n and $\xi_n = \psi_n + i\chi_n$. $(')$ denotes their first derivatives. The functions with the subscript w are their

DOI: 10.1021/acsphotonics.8b01251
ACS Photonics XXXX, XXX, XXX−XXX

generalization to a general complex order, defined explicitly by ref 11

$$\psi_w(z) \equiv (\pi z/2)^{1/2} J_\tau(z) \tag{7}$$

$$\chi_w(z) \equiv (\pi z/2)^{1/2} Y_\tau(z) \tag{8}$$

$$\xi_w(z) \equiv \psi_w(z) + i\chi_w(z) \tag{9}$$

where

$$\tau = w + 1/2 \tag{10}$$

$$w(n) = \sqrt{\frac{1}{4} + \frac{\varepsilon_t}{\varepsilon_n}(n^2 + n)} - \frac{1}{2} \tag{11}$$

J_τ and Y_τ are Bessel functions of the first and second kinds.[35] w is a function of n and will, in general, be complex if ε_t or ε_n is complex, for example, for absorbing or conducting materials in the shell or if one is negative, as found in hyperbolic materials. w may also be wavelength-dependent. If $\varepsilon_t = \varepsilon_n$, then $w(n) = n$ and all the expressions reduce to the isotropic case as expected. It is worth highlighting that the definition for χ_w is here different to that chosen in ref 11 in terms of $J_{-\tau}$. This choice does not affect the Mie coefficients, but ensures that the Wronskian identity $\psi_w\chi_w' - \psi_w'\chi_w = 1$ is fulfilled. This expression will be used for simplifications in the next section.

THIN ANISOTROPIC SHELL APPROXIMATION (TASA)

To simplify calculations, facilitate further theoretical developments, and foster the adoption of the general theory presented in the previous section, it is useful to derive simpler expressions under specific assumptions. For example, Roth and Dignam provided expressions in the quasi-static limit, that is, for particle sizes much smaller than the wavelength to lowest orders in the size parameter.[11] More accurate expressions, including higher order corrections, have similarly been obtained for nanoshells made of isotropic materials.[36] Lange and Aragon found a simple approximation in the special case of bubbles and vesicles (where $\varepsilon_c = \varepsilon_m$) in the limit of thin shells,[33] which was later extended to thicker shell by including the next order corrections.[37]

Here we will derive the lowest-order approximation for thin-shells in the more general case where the core is different from the outside medium, $\varepsilon_c \neq \varepsilon_m$, with ε_c possibly complex. Defining $\delta = x - y = k_m d$, we are therefore searching for the approximation in the limit $\delta \ll x, y$. We can view the Mie coefficients as functions of y and x, or equivalently of y and δ. For the thin-shell approximation, we can then use a Taylor expansion to the first order in δ, which gives, for example, for Δ_n:

$$\Delta_n(y, x) \approx \Delta_n(y, x = y) + \delta \left.\frac{\partial \Delta_n}{\partial x}\right|_{x=y} \tag{12}$$

The full derivations for $\Gamma_n(\delta)$ and $\Delta_n(\delta)$ are provided in section S2 (Supporting Information). It is worth noting that this involves some useful identities to simplify the complex orders of the Riccati-Bessel functions, which are given and proved in section S1. The final results are

$$\Delta_n(y, \delta) = -\frac{N_{2n}}{D_{2n}} - \delta\left(\frac{N_{2n}'}{D_{2n}} - \frac{N_{2n}D_{2n}'}{(D_{2n})^2}\right) \tag{13}$$

where

$$\begin{aligned}
N_{2n} &= s_c\psi_n'(y)\psi_n(s_c y) - \psi_n(y)\psi_n'(s_c y)\\
D_{2n} &= s_c\xi_n'(y)\psi_n(s_c y) - \xi_n(y)\psi_n'(s_c y)\\
N_{2n}' &= \frac{s_c n(n+1)}{y^2}\left(1 - \frac{\varepsilon_t}{\varepsilon_n s_t^2}\right)\psi_n(y)\psi_n(s_c y) + (s_t^2 - 1)\psi_n'(y)\psi_n'(s_c y)\\
D_{2n}' &= \frac{s_c n(n+1)}{y^2}\left(1 - \frac{\varepsilon_t}{\varepsilon_n s_t^2}\right)\xi_n(y)\psi_n(s_c y) + (s_t^2 - 1)\xi_n'(y)\psi_n'(s_c y)
\end{aligned} \tag{14}$$

and

$$\Gamma_n(y, \delta) = -\frac{N_{1n}}{D_{1n}} - \delta\left(\frac{N_{1n}'}{D_{1n}} - \frac{N_{1n}D_{1n}'}{(D_{1n})^2}\right) \tag{15}$$

where,

$$\begin{aligned}
N_{1n} &= s_c\psi_n(y)\psi_n'(s_c y) - \psi_n'(y)\psi_n(s_c y)\\
D_{1n} &= s_c\xi_n(y)\psi_n'(s_c y) - \xi_n'(y)\psi_n(s_c y)\\
N_{1n}' &= (1 - s_t^2)\psi_n(y)\psi_n(s_c y)\\
D_{1n}' &= (1 - s_t^2)\xi_n(y)\psi_n(s_c y)
\end{aligned} \tag{16}$$

We note that for $\delta = 0$, we recover the expressions of standard Mie theory for the core only, as expected. The most important outcome of this first-order expansion is that the resulting expressions for Γ_n and Δ_n only involve spherical Bessel functions of order n, as in standard Mie theory. The complex-order Bessel functions are no longer required in this approximation. This is the same as was obtained in the thin-shell approximation for bubbles.[33] In fact, if we set $\varepsilon_m = \varepsilon_c (s_c = 1)$, then our expressions further simplify to

$$\Gamma_n(\delta) = i\delta(1 - s_t^2)\{\psi_n(y)\}^2 \tag{17}$$

$$\Delta_n(\delta) = i\delta\frac{n(n+1)}{y^2}\left(\frac{\varepsilon_t}{s_t^2\varepsilon_n} - 1\right)\{\psi_n(y)\}^2 + i\delta(1 - s_t^2)\{\psi_n'(y)\}^2 \tag{18}$$

which are exactly the same expressions as (3.16 and 3.17) in ref 33, as expected.

MICROSCOPIC AND EFFECTIVE MEDIUM MODELS FOR AN ANISOTROPIC LAYER OF ADSORBED MOLECULES

In order to illustrate the range of validity and usefulness of this thin-shell approximation, we will focus on a specific system: a dye-coated metallic nanosphere. Measurements of the extinction or absorption properties have already been performed on such structures.[20] They are relevant to many experimental techniques, including surface-enhanced Raman spectroscopy (SERS) or fluorescence[6] and to studies of molecular/plasmon resonance interactions. It is also well-known that the adsorption orientation of molecules on a metallic nanoparticles can significantly affect its optical properties; this for example results in the surface selection rules in SERS.[6,38−40]

For an isolated dye on a metallic nanosphere, its optical properties can be simply understood using a microscopic description of the dye and standard Mie theory for the nanosphere.[6] For a given incident field $\mathbf{E}_0$, the local field at the dye position $\mathbf{E}_{loc}$ can be computed from Mie theory and decomposed into a sum of its normal, $\mathbf{E}_{loc}^{\perp}$, and tangential, $\mathbf{E}_{loc}^{\parallel}$,

DOI: 10.1021/acsphotonics.8b01251
ACS Photonics XXXX, XXX, XXX−XXX

components (with respect to the sphere surface). For a dye polarizability tensor $\underline{\alpha}$, the local field induces an oscillating dipole $\mathbf{p} = \underline{\alpha}\mathbf{E}_{loc}$. We will restrict to the common situation where the dye polarizability tensor is uniaxial along the main molecular axis with unit vector $\mathbf{e}_d$ and characterized by a scalar polarizability along this axis α_{zz}. The induced dipole is then given by $\mathbf{p} = \alpha_{zz}(\mathbf{E}_{loc} \times \mathbf{e}_d)\mathbf{e}_d$. The power absorbed and corresponding absorption cross-section for this induced dipole follow from standard electromagnetic theory, which including the microscopic local-field correction gives (ref 6, eqs 4.77 and 4.79):

$$\sigma_{abs} = \frac{2\pi}{\lambda\sqrt{\varepsilon_m}}(L_m)^2\frac{|\mathbf{e}_d\cdot\mathbf{E}_{loc}|^2}{|\mathbf{E}_0|^2}\frac{\mathrm{Im}(\alpha_{zz})}{\varepsilon_0} \tag{19}$$

where

$$L_m = \frac{\varepsilon_m + 2}{3} \tag{20}$$

is the microscopic local-field correction factor.[6,41,42] $L_m = 1$ for air or vacuum and is often ignored in theoretical treatments, but is important in order to be relevant to experiments in solution; it is therefore included explicitly here and in the effective medium model discussed below. Note that eq 19 could also be expressed in terms of the bare dye cross-section σ^0_{dye} (in the same medium):

$$\sigma_{abs} = \sigma^0_{dye}\frac{3|\mathbf{e}_d\cdot\mathbf{E}_{loc}|^2}{|\mathbf{E}_0|^2} \tag{21}$$

where

$$\sigma^0_{dye} = \frac{2\pi}{\lambda\sqrt{\varepsilon_m}}(L_m)^2\frac{\mathrm{Im}(\alpha_{zz})}{3\varepsilon_0} \tag{22}$$

The factor of 1/3 above arises from the orientation averaging of the dye in solution.

The cross-section was derived for a single molecule, but can be extended to a collection of N randomly adsorbed molecules by surface-averaging of the local field. To further simplify, we will consider three types of adsorption geometry relevant to experiments and depicted in Figure 2. For random orientation

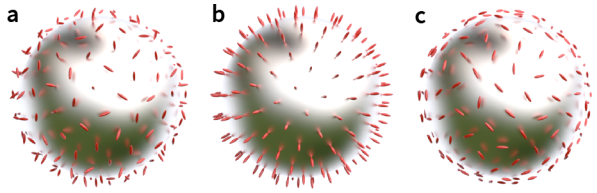

Figure 2. Three possible adsorption orientations of uniaxial dyes relevant to experiments: (a) fully random orientation denoted *, (b) perpendicular or radial denoted ⊥, and (c) random in-plane (tangential) orientations denoted ∥. In all three cases, we assume the dyes to be adsorbed uniformly on the sphere surface.

(*), the dye-layer response becomes isotropic, while for radial (⊥) and in-plane (∥) orientations, the response should be anisotropic. In all three cases, the absorption cross-section for N dyes can be expressed as

$$C_{abs}(\lambda) = N\sigma^0_{dye}M(\lambda) \tag{23}$$

where the absorption enhancement factor $M(\lambda)$ is wavelength-dependent and given for each case as

$$\begin{aligned} M^* &= \frac{\langle|\mathbf{E}_{loc}|^2\rangle}{|\mathbf{E}_0|^2}, \\ M^\perp &= \frac{3\langle|\mathbf{E}^\perp_{loc}|^2\rangle}{|\mathbf{E}_0|^2}, \\ M^\parallel &= \frac{3\langle|\mathbf{E}^\parallel_{loc}|^2\rangle}{2|\mathbf{E}_0|^2} \end{aligned} \tag{24}$$

$\langle\cdot\rangle$ refers to averaging over the surface of the sphere (since the local field is not uniform). Averaging over the possible orientations of the dyes results in an additional factor of 1/3 (*), 1 (⊥), and 1/2 (∥); these are multiplied by the existing factor of 3 in eq 21. Note that, in order to compare to experiments, one should also add the contribution of the core (calculated from Mie theory) to obtain the absorption cross-section of the coated sphere. In practice, especially at low dye coverage, one can also measure the bare sphere (with no coating) separately and subtract it from the coated sphere spectrum to reveal the experimental differential absorption spectrum, as explained in ref 20. Within the approximations of the microscopic model, this differential absorption spectrum is then given by $C_{abs}(\lambda)$ as in eq 23. It should be noted that this microscopic model does not take into account the possible effect of the dye layer onto the particle response nor of one dye onto the others (dye/dye interactions).

The effective medium approximation[28,29,43] replaces the discrete dye layer of given coverage ρ (dye/nm^2) by a homogeneous shell of thickness d, from which the volume V_s and volumic dye concentration $c_d = N/V_s \approx \rho/d$ can be inferred. In the general case, local field corrections arising from dye/dye interactions should be taken into account,[44] and their inclusion is a standard feature of the effective medium approximation for a 3D isotropic medium.[20,28,29] Generalizing those to a 2D anisotropic medium is outside the scope of this work, so we will neglect them here and only consider the much simpler dilute limit. An effective dielectric function for the homogeneous shell can then be defined following a standard approach. In the case of fully random orientation, the effective dielectric function is isotropic and given in the dilute case by[29]

$$\varepsilon^* = \varepsilon_m + c_d\frac{(L_m)^2\alpha_{zz}}{3\varepsilon_0} \tag{25}$$

In the dilute regime, we may use the microscopic model (eq 24) as a guide to generalize this to the anisotropic cases. For radially oriented molecules, we have

$$\begin{aligned} \varepsilon_n^\perp &= \varepsilon_m + c_d\frac{(L_m)^2\alpha_{zz}}{\varepsilon_0}, \\ \varepsilon_t^\perp &= \varepsilon_m \end{aligned} \tag{26}$$

For randomly oriented in-plane molecules, we have

$$\begin{aligned} \varepsilon_n^\parallel &= \varepsilon_m, \\ \varepsilon_t^\parallel &= \varepsilon_m + c_d\frac{(L_m)^2\alpha_{zz}}{2\varepsilon_0} \end{aligned} \tag{27}$$

Note that, in the dilute case considered here (e.g., for small ρ), the predictions are independent of the thickness d as long as it is small (with respect to the other dimensions, sphere radius

DOI: 10.1021/acsphotonics.8b01251
ACS Photonics XXXX, XXX, XXX−XXX

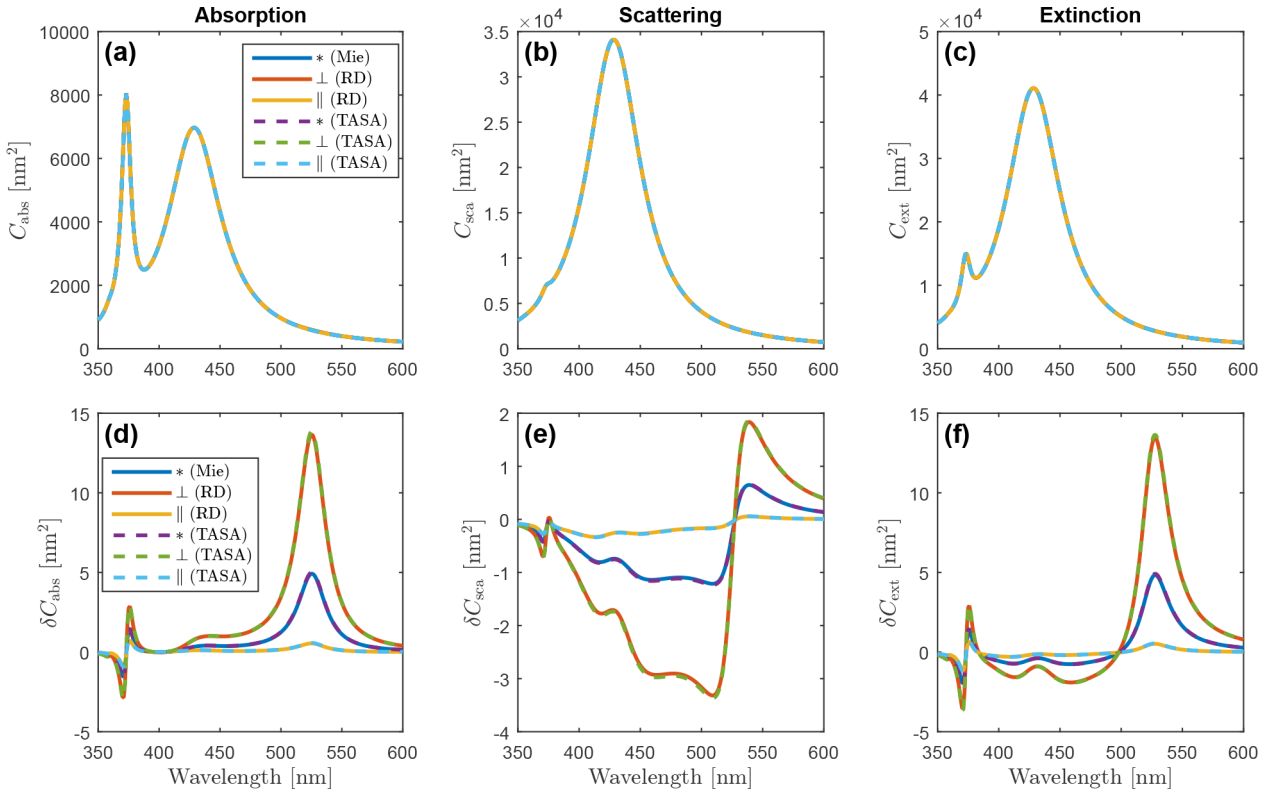

Figure 3. Mie scattering predictions for a silver sphere of radius a = 30 nm in water, coated with a d = 0.3 nm dye layer of low coverage ρ = 0.001 nm^2 in the effective medium approximation for the three cases of Figure 2 (see eqs 25−27). In the two anisotropic cases, we compare the results of the full theory of Roth and Dignam (RD) with our thin-shell approximation (TASA). The top row shows the absorption (a), scattering (b), and extinction (c) cross sections, which are indistinguishable in all six cases, as they are strongly dominated by the response of the silver sphere. We therefore show in the bottom row (d−f) the corresponding differential cross sections with the bare sphere response (calculated from standard Mie theory) subtracted.

and wavelength). In the following, we will set d = 0.3 nm, unless otherwise stated.

MODEL VALIDATION AND APPLICATION

Using the anisotropic effective dielectric functions just derived, we can now predict the optical properties of a dye-coated nanosphere and compare the results of the different models presented: Roth and Dignam's Mie theory for anisotropic shells (RD), our simpler thin anisotropic shell approximation (TASA), and the microscopic model (MM) given in the previous section. We choose to focus on a 30 nm radius silver sphere with a dielectric function, as given in ref 6. All calculations are performed in Matlab and are adapted from the SPlaC codes,[45] with new routines developed to calculate Bessel functions of complex orders. The embedding medium is chosen as water ($\varepsilon_m = 1.33^2$) to be more relevant to experiments. For the dye polarizability, we use a simple Lorentz oscillator model with parameters matching the experimentally measured optical properties of the main absorption peak of Rhodamine 6G, explicitly (using the notation of ref 29):

$$\alpha_{zz}(\lambda) = 3\alpha_d = 3\alpha_\infty + \frac{3\alpha_1\lambda_1}{\mu_1}\left[\frac{1}{1 - \frac{\lambda_1^2}{\lambda^2} - i\frac{\lambda_1^2}{\lambda\mu_1}} - 1\right] \quad (28)$$

with $\alpha_\infty = 3.2 \times 10^{-39}$ [SI], $\alpha_1 = 1.92 \times 10^{-38}$ [SI], $\lambda_1 = 526$ nm, $\mu_1 = 10^4$ nm. Those were obtained from the experimentally measured absorption cross-section in water, taking into account the local field correction factor.[46]

We first compare in Figure 3 the results of the full anisotropic theory and the thin-shell approximation for dye-coated silver spheres using the dilute effective medium model in the three cases discussed earlier: *, ⊥, ∥ (see also Figure S1 for a similar plot with a dielectric sphere). We set here a low dye coverage of ρ = 0.001 nm^{-2} and will discuss later concentration effects. The absorption, scattering, and extinction spectra are shown for reference (a−c) but do not reveal clearly the shell properties and the differences between the models, as they are strongly dominated by the sphere response. We therefore focus on the differential absorption, scattering, and extinction spectra (d−f). These are still barely distinguishable in all three cases: excluding the regions of zero-crossing, the relative error is of the order of 2% for * and ⊥ cases and 5% for ∥. The accuracy of the thin-shell approximation is further investigated in Figure S2 for larger shell thicknesses up to 5 nm. For a 1 nm shell, for example, the relative error increases to ≈6% for * and ⊥ and ≈15% for ∥. These results, along with more extensive testing not shown, confirm the validity of the thin-shell approximation and suggest that it can be used safely in all the cases considered here (with a 0.3 nm shell, i.e., 1:100 shell-to-radius ratio) and even up to 1 nm, that is, a 1:30 shell-to-radius ratio. We therefore use it in the following to discuss the spectral changes predicted for each situation. To further explain the observed spectra, we compare in Figure 4 these results to the microscopic model predictions. The two models agree well in the dye absorption region,

DOI: 10.1021/acsphotonics.8b01251
ACS Photonics XXXX, XXX, XXX−XXX

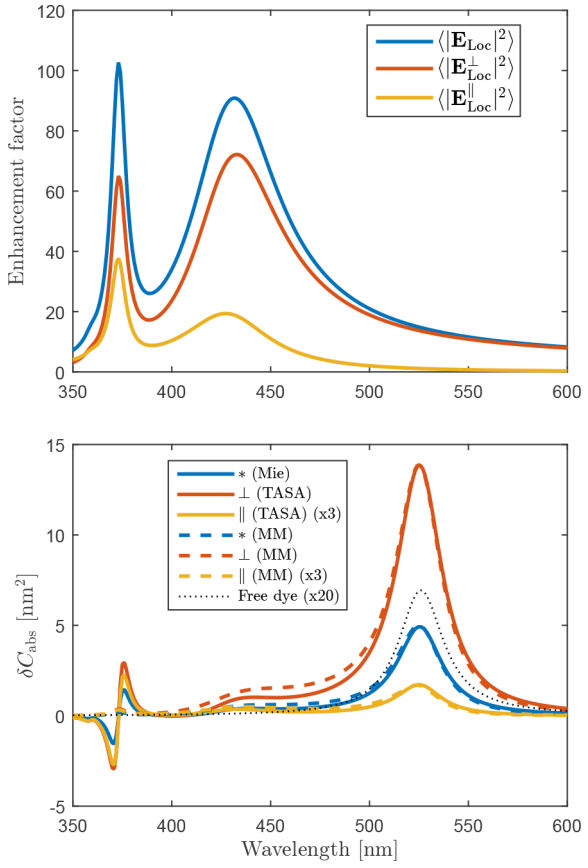

Figure 4. Comparison with the microscopic model (MM). (top) Surface-averaged local field enhancement factors: the peak at 430 nm correspond to the main dipolar plasmon resonance for the silver sphere in water, while the sharper 375 nm peak is the quadrupolar plasmon resonance. (bottom) Differential absorption cross sections, as predicted from the models considered here: full anisotropic Mie solution (RD), thin-shell approximation (TASA) in the dilute effective medium approximation, and microscopic model (MM). The three orientations of Figure 2 are considered: random (*), out-of-plane (⊥), and random in-plane (∥).

lending further support to the anisotropic effective dielectric functions defined in eqs 25−27.

We now discuss in more detail the orientation dependence evidenced in Figures 3 and 4. First, we observe a large difference in the magnitude of the dye absorption spectrum. For a silver sphere, the absorption is expected to be enhanced by a factor M because of the plasmon resonance, which peaks at 430 nm but extends further in the red. For example, $M^* = \langle|\mathbf{E}_{\mathrm{loc}}|^2/|E_0|^2\rangle$ is still of the order of ∼15 at the peak absorption of the dye at 526 nm. It is clear that this absorption enhancement is orientation-dependent and much stronger (respectively weaker) at ∼40 (respectively ∼1.6) for molecular axis perpendicular (respectively parallel) to the surface, as is well-known qualitatively in the context of surface-enhanced spectroscopy. The anisotropic effective shell models fully predict and quantify this effect. They moreover predict two phenomena that are not captured by the microscopic model. First, we see in Figure 4 that the TASA prediction differs from the microscopic model in the region of the plasmon resonances of the sphere (430 nm for the main resonance and 375 nm for the quadrupolar resonance). The TASA differential absorbance spectra show evidence for the shift in the plasmon resonances, especially clear around the sharper quadrupolar resonance, as evidenced by the characteristic derivative-like spectral shape. These shifts are again expected and well documented,[14] but how dye-orientation may affect them has not been discussed. The effective shell model provides a simple tool to study this orientation dependence. The predicted plasmon resonance shifts are smaller for parallel orientation compared to perpendicular, but the discrepancy is much less pronounced than that observed for the dye absorption enhancement. These predictions can also be extended to the other properties, differential scattering and extinction, which are not covered within the microscopic model. For example, the plasmon resonance shifts are also observed in differential extinction (Figure 3), but the spectra are more complicated as the dye layer also induces a significant reduction in scattering.

The second aspect that is not captured by the microscopic model is the effect of dye coverage. The coverage-dependent predictions of the anisotropic Mie model (within the TASA) are illustrated in Figure 5. As the dye concentration is increased, shifts in the dye resonance are predicted by the anisotropic Mie models and depend on the dye orientation: a blueshift for random orientation, a more pronounced blueshift for ⊥, and virtually no change for ∥, even at significantly higher coverage. The ⊥ spectral shifts are similar to those arising from the dye/dye interactions and are expected at higher concentrations, as studied in ref 29. Interestingly, the redshift that is expected for the ∥ orientation case is not observed here. We attribute this to the fact that our dilute effective medium shell model does not include local field corrections due to other dyes within the shell layer, which are in principle important at high concentration. These corrections could be included but they cannot be simply based on the Clausius-Mossotti relation as in isotropic media[20,29] since the anisotropic response must be taken into account in calculating the local fields arising from dye/dye interactions. The formalism for this has been laid out in the past,[44,47] but its implementation is outside the scope of this work and will be discussed elsewhere.

CONCLUSION

In summary, we have derived expressions for the Mie coefficients of the isotropic-core/anisotropic-shell scattering problem in the thin-shell approximation. The range of validity of this approximation was checked against the full anisotropic theory and shown to be particularly suited to the case of an adsorbed molecular layer on a nanoparticle. The main advantage of this approximation is that the resulting expressions are of comparable complexity to those of Mie theory for isotropic materials. In particular, they no longer require the computation of complex-order Bessel functions as in the anisotropic Mie theory. We believe this simplified theory will find application in many areas where the orientation of adsorbates result in an anisotropic optical response. We illustrated its usefulness by modeling the optical properties of adsorbed dye layers on metallic nanoparticles, which are relevant to a number of recent dye/plasmon coupling studies. For this, we proposed a simple generalization of the dilute effective medium theory to anisotropic cases. The resulting theory provides an insight into dye-orientation effects on the optical properties of dye-coated nanoparticles at low coverage. To simplify the interpretations and discussions, we here discussed the case where the plasmon and dye resonances do not overlap, but the model would also readily apply to the important case where those resonances interact. Another

DOI: 10.1021/acsphotonics.8b01251
ACS Photonics XXXX, XXX, XXX−XXX

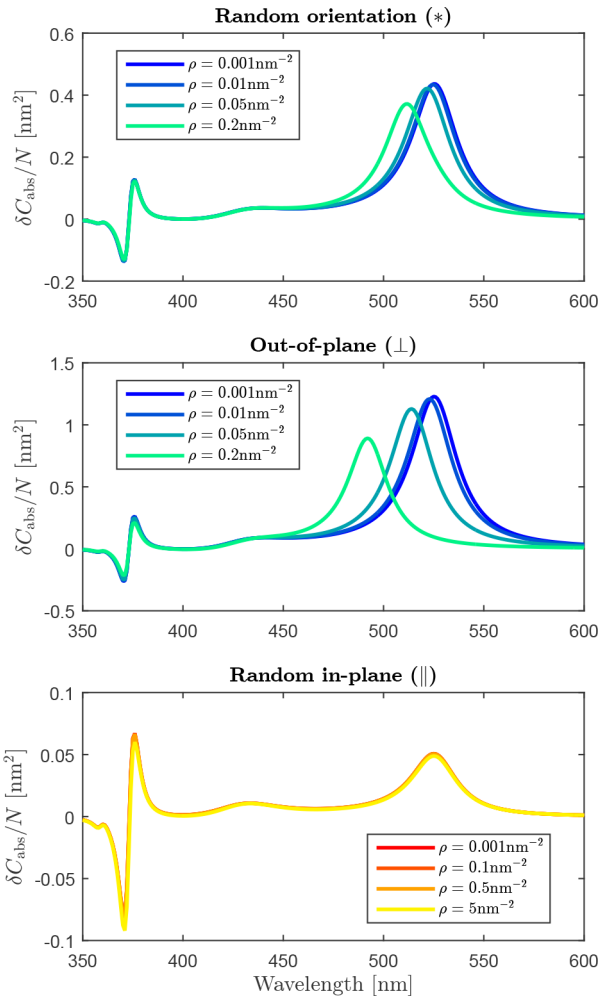

Figure 5. Dye-coverage dependence of the differential absorption cross-section as predicted from the Mie anisotropic model (in the thin-shell approximation) for the three cases of effective shell model: *, ⊥, and || (see eqs 25−27). Note that the range of coverage considered for the parallel case is larger than the other two, but no spectral shift is observed. Note also that the spectra are normalized by the number of molecules per nanoparticle. The unchanged derivative-like shape around 375 nm indicate that the magnitude of the redshift of the quadrupolar plasmon resonance is proportional to the dye coverage (and remains small in all cases considered here).

natural extension of this work will be to incorporate local field effects akin to the Clausius-Mossotti correction into the anisotropic effective medium shell model. Dye−dye interactions and orientation effects at high concentration (close to monolayer coverage) and how they relate to plasmon resonance coupling could then be studied in detail with anisotropic Mie theory.

■ ASSOCIATED CONTENT

Supporting Information

The Supporting Information is available free of charge on the ACS Publications website at DOI: 10.1021/acsphotonics.8b01251.

Detailed derivations of thin-anisotropic shell approximation expressions and additional Figures S1 and S2 (PDF).

■ AUTHOR INFORMATION

Corresponding Authors

*E-mail: chhayly.tang@vuw.ac.nz.
*E-mail: eric.leru@vuw.ac.nz.

ORCID

Baptiste Auguié: 0000-0002-2749-5715
Eric C. Le Ru: 0000-0002-3052-9947

Notes

The authors declare no competing financial interest.

■ ACKNOWLEDGMENTS

The authors thank the Royal Society Te Apārangi (New Zealand) for support through a Rutherford Discovery Fellowship (B.A.) and a Marsden Grant (E.C.L.R.).

■ REFERENCES

(1) Bohren, C. F.; Huffman, D. R. *Absorption and Scattering of Light by Small Particles*; John Wiley & Sons Inc.: New York, 1983.
(2) Novotny, L.; Hecht, B. *Principles of Nano-Optics*; Cambridge University Press: Cambridge, 2006.
(3) Teitler, S.; Henvis, B. W. Refraction in Stratified, Anisotropic Media*. *J. Opt. Soc. Am.* **1970**, *60*, 830−834.
(4) Kerker, M. *The Scattering of Light and Other Electromagnetic Radiation*; Academic Press: New York, 1969.
(5) Kerker, M.; Wang, D.-S.; Chew, H. *Appl. Opt.* **1980**, *19*, 4159−4174.
(6) Le Ru, E. C.; Etchegoin, P. G. *Principles of Surface Enhanced Raman Spectroscopy and Related Plasmonic Effects*; Elsevier: Amsterdam, 2009.
(7) Averitt, R. D.; Sarkar, D.; Halas, N. J. Plasmon Resonance Shifts of Au-Coated Au_2S Nanoshells: Insight into Multicomponent Nanoparticle Growth. *Phys. Rev. Lett.* **1997**, *78*, 4217−4220.
(8) Prodan, E.; Nordlander, P. Structural Tunability of the Plasmon Resonances in Metallic Nanoshells. *Nano Lett.* **2003**, *3*, 543−547.
(9) Fofang, N. T.; Park, T.-H.; Neumann, O.; Mirin, N. A.; Nordlander, P.; Halas, N. J. Plexcitonic nanoparticles: Plasmon-exciton coupling in nanoshell-J-aggregate complexes. *Nano Lett.* **2008**, *8*, 3481−3487.
(10) Contreras-Cáceres, R.; Pacifico, J.; Pastoriza-Santos, I.; Pérez-Juste, J.; Fernández-Barbero, A.; Liz-Marzán, L. M. Au@pNIPAM Thermosensitive Nanostructures: Control over Shell Cross-linking, Overall Dimensions, and Core Growth. *Adv. Funct. Mater.* **2009**, *19*, 3070−3076.
(11) Roth, J.; Dignam, M. J. Scattering and extinction cross sections for a spherical particle coated with an oriented molecular layer. *J. Opt. Soc. Am.* **1973**, *63*, 308−311.
(12) Qiu, C. W.; Gao, L.; Joannopoulos, J. D.; Soljacic, M. Light scattering from anisotropic particles: propagation, localization, and nonlinearity. *Laser Photonics Rev.* **2010**, *4*, 268−282.
(13) Wallén, H.; Kettunen, H.; Sihvola, A. Anomalous absorption, plasmonic resonances, and invisibility of radially anisotropic spheres. *Radio Sci.* **2015**, *50*, 18−28.
(14) Zhao, J.; Jensen, L.; Sung, J.; Zou, S.; Schatz, G. C.; Van Duyne, R. P. Interaction of plasmon and molecular resonances for rhodamine 6G adsorbed on silver nanoparticles. *J. Am. Chem. Soc.* **2007**, *129*, 7647−7656.
(15) Ni, W.; et al. Observing plasmonic-molecular resonance coupling on single gold nanorods. *Nano Lett.* **2010**, *10*, 77−84.
(16) Ni, W.; et al. Effects of dyes, gold nanocrystals, pH, and metal ions on plasmonic and molecular resonance coupling. *J. Am. Chem. Soc.* **2010**, *132*, 4806−4814.
(17) Zengin, G.; et al. Approaching the strong coupling limit in single plasmonic nanorods interacting with J-aggregates. *Sci. Rep.* **2013**, *3*, 3074.

DOI: 10.1021/acsphotonics.8b01251
ACS Photonics XXXX, XXX, XXX−XXX

(18) Antosiewicz, T. J.; Apell, S. P.; Shegai, T. Plasmon-exciton interactions in a core-shell geometry: From enhanced absorption to strong coupling. *ACS Photonics* **2014**, *1*, 454−463.
(19) Cacciola, A.; et al. Ultrastrong coupling of plasmons and excitons in a nanoshell. *ACS Nano* **2014**, *8*, 11483−11492.
(20) Darby, B. L.; Auguié, B.; Meyer, M.; Pantoja, A. E.; Le Ru, E. C. Modified optical absorption of molecules on metallic nanoparticles at sub-monolayer coverage. *Nat. Photonics* **2016**, *10*, 40−46.
(21) Santhosh, K.; Bitton, O.; Chuntonov, L.; Haran, G. Vacuum Rabi splitting in a plasmonic cavity at the single quantum emitter limit. *Nat. Commun.* **2016**, *7*, 11823.
(22) Zengin, G.; et al. Evaluating conditions for strong coupling between NP plasmons and organic dyes using scattering and absorption spectroscopy. *J. Phys. Chem. C* **2016**, *120*, 20588−20596.
(23) Simon, T.; et al. Exploring the Optical Nonlinearities of Plasmon-Exciton Hybrid Resonances in Coupled Colloidal Nanostructures. *J. Phys. Chem. C* **2016**, *120*, 12226−12233.
(24) Zhong, X.; et al. Waveguide and Plasmonic Absorption-Induced Transparency. *ACS Nano* **2016**, *10*, 4570−4578.
(25) Chikkaraddy, R.; et al. Single-molecule strong coupling at room temperature in plasmonic nanocavities. *Nature* **2016**, *535*, 127−130.
(26) Zengin, G.; et al. Realizing strong light−matter interactions between single-nanoparticle plasmons and molecular excitons at ambient conditions. *Phys. Rev. Lett.* **2015**, *114*, 157401.
(27) Wang, H.; et al. Dynamics of Strong Coupling between J-Aggregates and Surface Plasmon Polaritons in Subwavelength Hole Arrays. *Adv. Funct. Mater.* **2016**, *26*, 6198−6205.
(28) Aspnes, D. E. Local-field effects and effective-medium theory: A microscopic perspective. *Am. J. Phys.* **1982**, *50*, 704−709.
(29) Auguié, B.; Le Ru, E. C. Optical Absorption of Dye Molecules in a Spherical Shell Geometry. *J. Phys. Chem. C* **2018**, *122*, 19110−19115.
(30) Ambjörnsson, T.; Mukhopadhyay, G.; Apell, S. P.; Käll, M. Resonant coupling between localized plasmons and anisotropic molecular coatings in ellipsoidal metal nanoparticles. *Phys. Rev. B: Condens. Matter Mater. Phys.* **2006**, *73*, 085412.
(31) Ambjörnsson, T.; Mukhopadhyay, G. Dipolar response of an ellipsoidal particle with an anisotropic coating. *J. Phys. A: Math. Gen.* **2003**, *36*, 10651.
(32) Ambjörnsson, T.; Apell, S. P.; Mukhopadhyay, G. Electromagnetic response of a dipole-coupled ellipsoidal bilayer. *Phys. Rev. E* **2004**, *69*, 031914.
(33) Lange, B.; Aragón, S. R. Mie scattering from thin anisotropic spherical shells. *J. Chem. Phys.* **1990**, *92*, 4643−4650.
(34) Rimpilainen, T.; Wallen, H.; Kettunen, H.; Sihvola, A. Electrical Response of Systropic Sphere. *IEEE Trans. Antennas Propag.* **2012**, *60*, 5348−5355.
(35) Abramowitz, M., Stegun, I. A., Eds. *Handbook of Mathematical Functions*; Dover: New York, 1972.
(36) Schebarchov, D.; Auguié, B.; Le Ru, E. C. Simple accurate approximations for the optical properties of metallic nanospheres and nanoshells. *Phys. Chem. Chem. Phys.* **2013**, *15*, 4233−4242.
(37) Hahn, D. K.; Aragón, S. R. Mie scattering from anisotropic thick spherical shells. *J. Chem. Phys.* **1994**, *101*, 8409−8417.
(38) Moskovits, M. Surface selection rules. *J. Chem. Phys.* **1982**, *77*, 4408−4416.
(39) Moskovits, M. Surface-enhanced spectroscopy. *Rev. Mod. Phys.* **1985**, *57*, 783−826.
(40) Le Ru, E. C.; et al. Experimental demonstration of surface selection rules for SERS on flat metallic surfaces. *Chem. Commun.* **2011**, *47*, 3903−3905.
(41) Polo, S. R.; Wilson, M. K. Infrared intensities in liquid and gas phases. *J. Chem. Phys.* **1955**, *23*, 2376.
(42) Eckhardt, G.; Wagner, W. G. On the calculation of absolute Raman scattering cross sections from Raman scattering coefficients. *J. Mol. Spectrosc.* **1966**, *19*, 407−411.
(43) Markel, V. A. Introduction to the Maxwell Garnett approximation: tutorial. *J. Opt. Soc. Am. A* **2016**, *33*, 1244−1256.
(44) Bagchi, A.; Barrera, R. G.; Fuchs, R. Local-field effect in optical reflectance from adsorbed overlayers. *Phys. Rev. B: Condens. Matter Mater. Phys.* **1982**, *25*, 7086−7096.
(45) Le Ru, E. C.; Etchegoin, P. G. SERS and Plasmonics Codes (SPlaC). Matlab codes freely available from http://www.vuw.ac.nz/raman/book/codes.aspx.
(46) Djorović, A.; Meyer, M.; Darby, B. L.; Le Ru, E. C. Accurate modeling of the polarizability of dyes for electromagnetic calculations. *ACS Omega* **2017**, *2*, 1804−1811.
(47) Dignam, M. J.; Moskovits, M. Optical properties of sub-monolayer molecular films. *J. Chem. Soc., Faraday Trans. 2* **1973**, *69*, 56−64.

DOI: 10.1021/acsphotonics.8b01251
ACS Photonics XXXX, XXX, XXX−XXX